Picosecond Transient Grating Experiments in Sodium Vapor: Velocity and Polarization Effects

Todd S. Rose, William L. Wilson, G. Wäckerle, and M. D. Fayer*

Department of Chemistry, Stanford University, Stanford, California 94305 *(Received: December 5, 1986)*

The picosecond transient grating technique is applied to the $^2S_{1/2} \rightarrow {}^2P_{1/2}$ and $^2P_{3/2}$ transitions in sodium vapor. A population grating is generated by using parallel polarization for the two excitation pulses. The signal decay is directly related to the velocity distribution of the atoms. When the polarizations of the excitation pulses are perpendicular, a polarization grating is formed, and oscillations corresponding to the ground- and excited-state hyperfine splittings are observed.

Recently, there has been considerable interest in the nonlinear optical properties of sodium vapor. Four-wave mixing (FWM) experiments have been performed in the frequency domain in order to obtain information concerning the third-order susceptibility

0022-3654/87/2091-1704$01.50/0

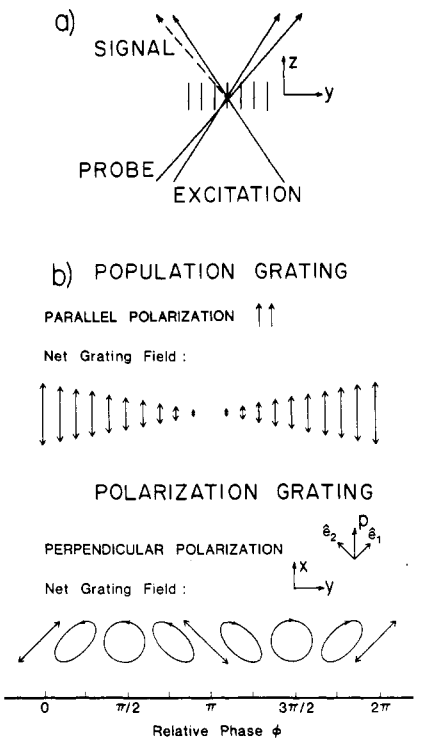

Figure 1. (a) Experimental geometry of the transient grating experiment. The excitation pulses, which propagate essentially in the $\hat{z}$ direction, for a grating with a wave vector along $\hat{y}$. (b) Spatial polarization dependence of the population and polarization gratings. The overall intensity of the $\vec{E}$ field is uniform in the latter situation, but the polarization varies from linear to circular. The usual analysis of a polarization grating involves the decomposition of the probe polarization, p, into the vectors $\hat{e}_1$ and $\hat{e}_2$. In the analysis of these experiments, however, the probe is decomposed into right and left circular components.

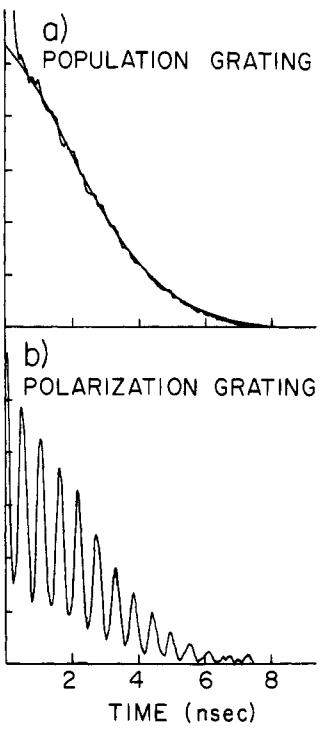

Figure 2. (a) Population grating (fringe spacing 12.2 μm, λ_{exc} = 5890 Å, λ_{probe} = 5896 Å, T_{exp} = 583 K, T_{fit} = 590 K). The signal decay is nonexponential and arises because of the spatial motion of the atoms. (b) Polarization grating (fringe spacing 12.2 μm, λ_{exc} = 5896 Å, λ_{probe} = 5890 Å). The oscillations in the signal arise because of the 1.77-GHz Na ground-state hyperfine splitting.

$\chi^{(3)}$[1-5] and the effect of collisions with buffer gases.[6] Time domain FWM experiments, such as the trilevel echo,[7] two-photon echo,[8] stimulated echo,[9] grating echo,[10] and backward photon echo,[11] have also been employed to study collisional relaxation as well as investigate the effects of pulsed incoherent light.[12] In this Letter we report picosecond transient grating measurements on sodium vapor and demonstrate that the gas-phase velocity distribution can be obtained. The effect of the excitation polarization on the time-dependent signal is also discussed.

In the experiments tunable picosecond pulses are generated by synchronously pumping two dye lasers with the second harmonic of an acousto-optically Q-switched and mode-locked Nd:YAG laser. The output of one dye laser is used to produce the excitation pulses, while that of the other is used to generate the probe. Thus, the probe and excitation wavelengths can be independently tuned into the upper or lower sodium D lines at 589.0 nm ($^2P_{3/2}$) and 589.6 nm ($^2P_{1/2}$), respectively. The tunable pulses are 18 ps in duration and have a bandwidth of 0.7 cm^{-1}. The excitation and probe pulse energies were independently attenuated until the form of the signal remained unchanged with further attenuation. The resulting energies are ~100 nJ and ~0.5 μJ for the excitation and probe, respectively. The spot sizes are ~200 μm. The probe is delayed from the time coincident excitation pulses with a mechanical delay line. The pressure of the sodium vapor in the cell is maintained at about 2×10^{-7} Torr. The experimental geometry is depicted in Figure 1.

A normal population grating is established by the interference of two crossed excitation pulses which have the same polarization. If the polarization of one of the interfering pulses is rotated by 90°, a polarization grating is generated (see Figure 1b). In this configuration the polarization of the diffracted signal is rotated 90° with respect to the probe. Typical results for a fringe spacing of 12.2 μm are shown in Figure 2.

The nonexponential decay seen in Figure 2a has been predicted[13] but not previously observed. The excitation is tuned into the $^2P_{3/2}$ manifold, while the probe is resonant with the $^2P_{1/2}$ manifold. In the absence of collisions, the decay can be shown to be the square of the Fourier transform of the atomic velocity distribution (along the grating wave vector) multiplied by a lifetime term. Here we are considering a sample in thermal equilibrium, so the velocities are described by a Maxwell–Boltzmann distribution, i.e., a Gaussian. The time-dependent signal is

$$S(t) = Ae^{-(\Delta t)^2 K_B T/m} e^{-2t/\tau} \quad (1)$$

where A is a constant dependent upon experimental parameters such as beam intensities and optical density, τ is the fluorescence lifetime (16 ns for Na), Δ is the magnitude of the grating wave

(1) Bloom, D. M.; Liao, P. F.; Economon, N. P. *Opt. Lett.* **1978**, *2*, 58.
(2) Humphrey, L. M.; Gordon, J. P.; Liao, P. F. *Opt. Lett.* **1980**, *5*, 56.
(3) Woerdman, J. P.; Schuurmans, M. F. H. *Opt. Lett.* **1981**, *6*, 239.
(4) Jabr, S. N.; Lam, L. K.; Hellwarth, R. W. *Phys. Rev. A* **1981**, *24*, 3264.
(5) Kumar, P. *Opt. Lett.* **1985**, *10*, 74.
(6) Rothberg, L. J.; Bloembergen, N. *Phys. Rev. A* **1984**, *30*, 820.
(7) Mossberg, T.; Flusberg, A.; Kachru, R.; Hartmann, S. R. *Phys. Rev. Lett.* **1977**, *39*, 1523.
(8) Flusberg, A.; Mossberg, T.; Kachru, R.; Hartmann, S. R. *Phys. Rev. Lett.* **1978**, *41*, 305.
(9) Mossberg, T.; Flusberg, A.; Kachru, R.; Hartmann, S. R. *Phys. Rev. Lett.* **1979**, *42*, 1665.
(10) Mossberg, T. W.; Kachru, R.; Whittaker, E.; Hartmann, S. R. *Phys. Rev. Lett.* **1979**, *43*, 851.
(11) (a) Fujita, M.; Nakatsuka, H.; Nakanishi, H.; Matsuoka, M. *Phys. Rev. Lett.* **1979**, *42*, 974. (b) Jain, R. K.; Tom, H. W. K.; Diels, J. C. In *Picosecond Phenomena, III*; Springer-Verlag: West Berlin, 1982; Springer Ser. Chem. Phys. Vol. 23, p 250.
(12) Beach, R.; DeBeer, D.; Hartmann, S. R. *Phys. Rev. A* **1985**, *32*, 3467.
(13) Rose, T. S.; Fayer, M. D. *Chem. Phys. Lett.* **1985**, *117*, 12.
(14) Grundevik, P.; Lundberg, H.; Maertensson, A. M.; Nystroem, K.; Svanberg, S. *J. Phys. B* **1979**, *12*, 2645.
(15) Ducas, T. W.; Littman, M. G.; Zimmerman, M. C. *Phys. Rev. Lett.* **1975**, *35*, 1752.
(16) Leuchs, G.; Smith, S. J.; Khawaja, E.; Walther, H. *Opt. Commun.* **1979**, *31*, 313.
(17) Rothenberg, J. E.; Grischkowsky, D. *Opt. Lett.* **1985**, *10*, 22.

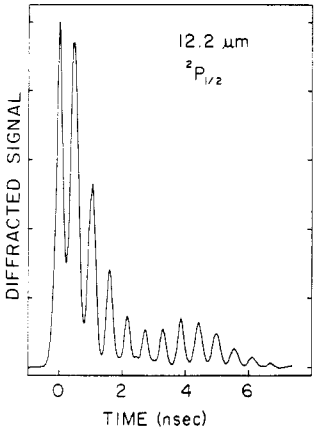

Figure 3. Na polarization grating. Both the probe and excitation pulses are tuned into the $^2P_{1/2}$ manifold. The high-frequency oscillations result from $^2S_{1/2}$ ground-state hyperfine splitting (1.77 GHz). A slower oscillation, which results in a peak at ~4 ns, is due to the excited-state hyperfine interaction (189 MHz). The oscillation from the excited hyperfine states is shifted by the Gaussian envelope decay to earlier time (fringe spacing 12.2 μm, T = 585 K).

vector ($\Delta = 2\pi/d$; d is the grating fringe spacing), K_B is Boltzmann's constant, and m is the mass. If the temperature is used as an adjustable parameter, the theoretical fit to the data in Figure 2a yields a temperature of 590 K as compared to a temperature of 583 K measured by a resistance thermometer in contact with the body of the sample cell. The data and the theoretical model are in excellent agreement. The major error in fitting the temperature arises from inaccuracies in determining the angle between the excitation beams which controls the fringe spacing. Given the procedures we employed, we estimate that the temperature can be determined to ±3%.

The results displayed in Figure 2a demonstrate a new approach to the measurement of gas-phase velocity distributions. The signal decays because the translational motion of the atoms destroys the spatial pattern which comprises the grating. Unlike a Doppler line width measurement, it is unnecessary to have high resolution or well-resolved spectral lines. Furthermore, transient grating spectroscopy is different from other velocity distribution measurement techniques, such as Doppler and FID spectroscopy, which rely on frequency effects. The grating provides a spatial yardstick, i.e., the grating fringe spacing, against which the motion of the atoms or molecules is measured. In previous experiments on I_2,[13] the direct determination of the velocity distribution was obscured by the collisional dynamics of the excited molecules. A detailed theoretical analysis of the earlier I_2 experiments, including velocity and collision effects, is forthcoming.[18] The Na results presented here clearly demonstrate that the basic theory for the evaluation of the grating signal in the absence of collisions is correct.

Figure 2b shows the results of the polarization grating experiment for excitation into the $^2P_{1/2}$ manifold and probing the $^2P_{3/2}$ manifold. (The temperature and fringe spacing are the same as in Figure 2a.) The signal oscillates with a frequency characteristic of the Na ground-state hyperfine splitting of 1.77 GHz.[6] The overall envelope of the signal still maintains a Gaussian shape. For the situation in which the probe and excitation are both tuned into the $^2P_{1/2}$ manifold, a second low-frequency modulation can be discerned (see Figure 3). This second frequency (189 MHz) corresponds to the hyperfine splitting of the excited $^2P_{1/2}$ manifold. The peak in the data from the excited-state hyperfine splitting is shifted somewhat to earlier time because of the decaying Gaussian envelope.

The consequence of changing the polarization of one of the excitation beams is quite dramatic. Polarization gratings have been analyzed for systems of randomly oriented molecules with well-defined transition dipole moments[19] or in terms of a Kerr effect.[20] In those experiments, the probe is resolved into the two linear vectors $\hat{e}_1$ and $\hat{e}_2$ shown in Figure 1b. For previously reported absorption polarization gratings, the regions that are oriented along $\hat{e}_1$ exhibit partial bleaching in that direction. The sample absorbs the $\hat{e}_2$ component of the probe more strongly than the $\hat{e}_1$ component. The opposite occurs for the grating region oriented along $\hat{e}_2$. The circular regions of the grating absorb the $\hat{e}_1$ and $\hat{e}_2$ components of the probe equally. The net result is that the two components of the probe experience two distinct gratings which are spatially shifted from each other along the grating wave vector by half a grating wavelength. Because of this spatial shift, the outgoing $\vec{E}$ fields from the two gratings are phase shifted by exactly 180°. This results in a rotation of the signal polarization by 90° with respect to a probe polarized parallel to one of the excitation polarizations.

For the sodium excited-state polarization grating, the vectorial analysis discussed above cannot explain the grating diffraction since an atom does not have an intrinsic direction for the transition dipole. However, if one decomposes the probe into right and left circularly polarized components (rcp and lcp), one can show that the rcp and lcp excited regions of the grating behave differently.[18] This results from the $\Delta M_F = +1$ or -1 selection rule for rcp and lcp light, respectively, where F is the combined nuclear and electronic angular momenta. (Here we have adopted the convention that rcp light exhibits clockwise rotation in a right-handed coordinate system when observed along the propagation axis, namely, the positive z axis. For consistency, we have chosen the selection rules such that $\Delta M_F = -1$ for lcp and $\Delta M_F = +1$ for rcp.) In the regions excited by rcp light, $\Delta M_F = +1$ transitions are partially bleached. Correspondingly, in the regions excited by lcp light, $\Delta M_F = -1$ transitions are partially bleached. The rcp and lcp excited regions of the grating interact differently with the right and left circular components of the linearly polarized probe. The linear parts of the grating are excited by both lcp and rcp light and, therefore, interact identically with both circularly polarized components of the probe. The two components of the probe experience two distinct gratings, spatially shifted by a half grating wavelength. This results in the observed 90° rotation of the signal polarization relative to the probe polarization.

The modulations in the signal intensity only appear in the polarization grating. These modulations persist well beyond the free induction decay time associated with the Doppler line width. Therefore, they cannot result from a macroscopic polarization beating that is induced by the excitation pulses. Quantum beats in other types of experiments on sodium vapor have been reported. Beats have been observed in fluorescence,[14] absorption,[15] and photoionization[16] experiments as well as nonlinear experiments,[11b,12,17,21] such as photon echoes and four-wave mixing. The free induction decay occurs on the time scale required for an atom to move on the order of an optical wavelength and gives rise to the coherence "spike" in the grating data at short time.

The oscillation in signal amplitude results from the formation of a coherent superposition of states on each atom by the excitation pulses. Because the oscillator strengths of the $^2S_{1/2} \rightarrow {}^2P_{3/2,1/2}$ transitions are large,[22] multiple interactions with the excitation field are possible if the excitation field is sufficiently intense. The Rabi angle for a 100-nJ, 18-ps excitation pulse focused to a spot size of 200 μm is approximately 7π. Since the Rabi frequency is so large, multiple transitions among all the hyperfine states (consistent with the selection rules) are possible. Thus, states from both ^2S hyperfine levels will be coupled via transitions to and from the ^2P manifold. Consequently, coherent superposition states consisting of the various hyperfine levels are produced via optical pumping. The preparation of coherent superposition states is a basic feature of nonlinear experiments. However, the oscillation in the polarization grating signal and its absence from the pop-

(18) Rose, T. S.; Wilson, W. L.; Wäckerle, G.; Fayer, M. D. *J. Phys. Chem.*, in press.
(19) Von Jena, A.; Lessing, H. E. *Opt. Quantum Electron.* **1979**, *11*, 419.
(20) Eyring, G.; Fayer, M. D. *J. Chem. Phys.* **1984**, *81*, 4314.
(21) Golub, J. E.; Mossberg, T. W. *J. Opt. Soc. Am. B: Opt. Phys.* **1986**, *3*, 554.
(22) Wiese, W. L.; Smith, M. W.; Miles, B. M. *Atomic Transition Probabilities*; National Bureau of Standards: Washington, DC, 1969; Vol. 2, p 2.

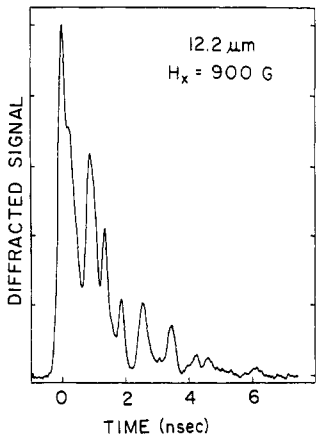

Figure 4. Na polarization grating. The sodium cell is placed in a static magnetic field of 900 G in the x direction. The field splits the degenerate hyperfine states, giving rise to additional frequency components in the grating signal. The temperature and fringe spacing are similar to that in Figure 2b.

ulation grating decay demonstrate that multiple interactions with the excitation field resulting in multilevel coherent superpositions is not sufficient to produce oscillations in the grating signal.

The oscillations in the polarization grating signal are caused by the time variation in the absorption probabilities experienced by the rcp and lcp components of the probe. This type of time-dependent absorption probability from a coherent superposition of states has been seen by Ducas et al.[15] in excited-state absorption experiments. The spatial separation of the rcp and lcp grating regions gives rise to spatially separated regions of rcp and lcp superposition states of Na. It can be shown that the phase relationships among the states involved in the superpositions result in oscillations in the diffracted signal.[18] On the other hand, the excitation conditions for the population grating produce only linearly polarized grating regions. These regions have different coherent superpositions with different phase relations than the rcp and lcp regions of the polarization grating. For the phase relationships which occur in the population grating, the oscillations in the signal can be shown to cancel.[18] As will be demonstrated in detail theoretically,[18] the overall result is that the observation of the coherence among the Na hyperfine levels is dependent upon the spatial separation of the lcp and rcp excitation regions in the polarization grating.

An interesting result occurs when the Na sample is placed in a magnetic field. The field has no effect on the population grating signal but significantly distorts the polarization grating oscillations (see Figure 4). In the absence of the field the hyperfine levels are $(2F + 1)$-fold degenerate. When the field is applied, the states are no longer degenerate due to the Zeeman effect. The additional splittings add extra frequency components to the grating signal, thereby complicating the appearance of the decay.

In this Letter we have demonstrated some aspects of the application of picosecond transient grating experiments to problems in gas-phase systems. The decay of the population grating is related to the Fourier transform of the velocity distribution of particles in the gas. The measurement can be used to study nonequilibrium systems as well as the thermal equilibrium situation presented here. For example, in a photofragmentation of a molecule AB to A + B, the probe could be tuned into one of the fragments and its velocity distribution directly measured. The polarization grating results demonstrate that high-resolution spectroscopic information can be obtained in situations where a $\Delta M = \pm 1$ selection rule occurs. Thus, examination of the dynamics of molecular rotational angular momentum states[23] should be possible with this approach. The information obtainable from grating experiments of this type, combined with the gratings spatial resolution and the coherent nature of the signal, will make this type of experiment useful in studying a variety of gas-phase problems including plasmas, flames,[24] and combustion.

Acknowledgment. This work was supported by the National Science Foundation, Division of Materials Research (Grant No. DMR 84-16343), and by the Office of Naval Research (Grant No. N00014-85-K-0409). Todd S. Rose thanks IBM for a graduate fellowship, William L. Wilson thanks AT&T Bell Laboratories for a graduate fellowship, and Gerhard Wäckerle thanks the Deutsche Forschungsgemeinschaft for partial support. We also thank Professor Sune Svanberg for very interesting conversations pertaining to this work.

(23) (a) Felker, P. M.; Baskin, J. S.; Zewail, A. H. *J. Phys. Chem.* **1986**, *90*, 724. (b) Felker, P. M.; Zewail, A. H., submitted for publication in *J. Chem. Phys.*

(24) Pender, J.; Hesselink, L. *Opt. Lett.* **1985**, *10*, 264.